SSRG International Journal of Mechanical Engineering
ISSN: 2348–8360 / https://doi.org/10.14445/23488360/IJME-V10I6P105

Volume 10 Issue 6, 29-38, June 2023

Original Article

Effect of Dynamic Coupling of Liquid Propellant Sloshing on the Response at Critical Locations of a Typical Liquid Propellant Rocket

S. Ganga[1], Deepthy S Nair[2], Rojan Mathew[3]

[1,2]*N.S.S College of Engineering, Akathethara, Palakkad, Kerala, India*
[3]*Scientist S.D., Engineering, STR, Vikram Sarabhai Space Center, Thiruvananthapuram, Kerala, India*

[1]*Corresponding Author : gangas25061999@gmail.com*

Received: 29 April 2023 Revised: 06 June 2023 Accepted: 18 June 2023 Published: 30 June 2023

Abstract *- Liquid propellant rocket utilizes an engine that uses liquid as a propellant. In liquid propellant rockets, fuel and oxidizer are pumped into the combustion chamber, where they get mixed and burned. Liquid hydrogen is mainly used as fuel, and liquid oxygen is used as an oxidizer. Slosh can occur with liquid propellants. Slosh acts as a tuned damper and helps in reducing the dynamic response of the vehicle. Slosh baffles in the tanks and intelligent control rules in the guidance system can be used to control this. A potential source of disturbance that is vital to the stability of spacecraft is the propellant slosh. A mechanical model of a spring-mass-damper system is commonly used to represent the sloshing dynamics. Modelling of a typical liquid propellant rocket propellant is done in MSC NASTRAN / PATRAN software. Dynamic characterization of liquid propellant rockets with and without propellant is carried out. Transient analysis on launch vehicles with propellant is carried out, and responses at critical locations are estimated. In this project, the structural dynamic characterization and response at critical locations of a liquid propellant rocket are conducted. The main objective of the project is to study the effect of coupling between the propellant sloshing and the vehicle modes.*

Keywords *- Coupling, Dynamic characterization, Liquid propellant rocket, Propellant sloshing, Transient analysis.*

1. Introduction

Jet propulsion is used for the propulsion of a rocket in the absence of the air around it. The high-speed exhaust powers a rocket. A rocket is powered by fuel, so it can fly in the vacuum of space. The force that propels any aircraft through the air is called thrust. The aircraft's propulsion system produces thrust.[26] Every thrust is produced through the application of Newton's third law of motion in some way, and different propulsion systems produce thrust in various ways. In any propulsion system, the system accelerates the working fluid, and the working fluid's reaction to this acceleration exerts a force on the system. Fuel and an oxygen source, known as an oxidizer, are combined and ignited in a combustion chamber to create a rocket engine. Hot exhaust from the combustion is sent through a nozzle to speed up the flow and create thrust. The hot exhaust created upon combustion serves as the rocket's accelerated gas or operating fluid. Liquid rockets and solid rockets are the two major types of rocket engines.0 In a liquid rocket, the fuel and the oxidizer, the two propellants, are stored separately as liquids and poured into the nozzle's combustion chamber, where burning takes place. The propellants are combined and crammed into a solid cylinder for a solid rocket. A liquid rocket's propulsion can be stopped by stopping the propellant flow, whereas a solid rocket's engine must be destroyed to be stopped. Due to the pumps and storage tanks, liquid rockets typically weigh more and require a more intricate design. Just before launch, the rocket is loaded with propellants. Liquid-propellant systems store the propellant in tanks outside the combustion chamber. The majority of these engines use liquid fuel and liquid oxidizers, which are transferred from their respective tanks through pumps. Propellers are then pumped into the engine in a way that ensures atomization and quick mixing after the pumps raise the pressure above the engine's operating pressure.[26]

A liquid rocket propulsion system typically consists of an engine, fuel tanks, and a vehicle frame to hold everything in place while connecting to the payload and launch pad (or vehicle). Considering that they function at low pressure, the fuel and oxidizer tanks are often made of very lightweight materials.[26]

The liquid has a free surface so that there will be a slosh dynamics problem, where there is a coupling of liquid i.e., liquid can interact with the container and drastically change the system's dynamics. Engineers in the fields of nuclear, civil, and aerospace still have a lot of concerns about the issue of liquid sloshing in moving or stationary containers.**Error! Reference source not found.** The slosh o

f propellant in the tanks and rockets of spacecraft are two significant examples. Spacecraft attitude destabilization may occur as a result of liquid sloshing in the tanks holding the propellants because it causes rapid energy loss during resonant modes. The liquid's free surface begins to slosh or oscillate when a container is put in motion.[2]

Here we are concerned with the effect of dynamic coupling of liquid propellant sloshing on the response at critical locations of a typical liquid propellant rocket. MSC PATRAN and MSC NASTRAN are used to model and analyze the propellent sloshing and typical rocket with liquid propellant. The main objective of the project is to study the effect of coupling between the propellant sloshing and the vehicle modes.

2. Objectives

The main objectives of the project are:

1. To develop the finite element model of a typical rocket with and without liquid propellant
2. To develop the finite element model of propellent sloshing.
3. To obtain the dynamic structural characterization of the liquid propellant rocket with and without propellant.
4. To obtain the response at the critical location of a liquid propellant rocket.
5. To study the effect of coupling between the propellant sloshing and the vehicle modes.

3. Methodology

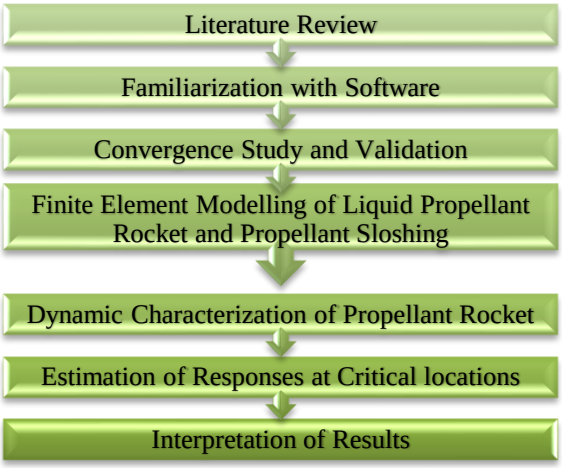

- Literature Review: Various journals and research papers were collected related to the problem, and a literature survey was conducted.
- Familiarization with software: PATRAN software is used for the modelling of launch vehicles and propellant slosh. And NASTRAN software is used for the dynamic analysis of launch vehicles.
- Validation: A comparison of mode shapes and frequencies of the cylindrical beam and shell of various diameters, heights and mesh sizes by keeping the aspect ratio the same was conducted.
- Finite Element Modelling of Liquid Propellant Rocket and Propellant Sloshing: Modelling of the launch vehicle with and without propellant in PATRAN software.
- Dynamic Characterization of Propellant Rocket: Modal analysis of a typical Propellant Rocket with and without propellant was done.
- Estimation of Responses at Critical Locations: Responses at critical locations of launch vehicles were made by transient analysis.
- Interpretation of Result: The coupling effect between the propellant sloshing and the vehicle modes was studied.

4. Validation

4.1. Convergence Study

Cylindrical beams and shells were modelled in PATRAN. Frequencies and mode shapes under different cases were cross-checked. The first comparison is checked by changing the height and keeping aspect ratios the same for both the beam and cylinder. The second is by changing the diameter, keeping aspect ratios the same for both beam and cylinder; the Third is by changing the mesh size of both beam and cylinder. Percentage differences in frequencies of first, second bending mode and first axial mode under different cases were checked.

It is seen that as height increased percentage difference in frequencies of the first bending mode, second bending mode, and axial mode decreased as per the first case. The cylindrical shell of 10-meter height and 1-meter diameter is taken to model the propellant tank as its percentage difference in frequencies of 1^{st}, 2^{nd} bending mode, and 1^{st} axial mode is less than 5%. It is seen that as the diameter decreased percentage difference in frequencies of the first bending mode, the second bending mode and the axial mode decreased for a mesh size of 0.05 as per the second case. As per the third case, it is seen that for two different mesh sizes, the first bending mode, second bending mode and axial mode remained the same for both beam and cylinder for both 0.05 and 0.01 mesh sizes.

From the analysis, it can be concluded that by keeping the diameter the same with increasing height, keeping the height same with decreasing diameter and varying the mesh size from 0.05 to 0.01, frequencies corresponding to the first bending mode, 2^{nd} bending mode and axial mode of both cylindrical beam and shell become almost same for increasing heights, with decreasing diameter and varying mesh size.

5. Finite Element Modelling

5.1. Typical Launch Vehicle Modelling

Launch vehicles are used to carry spacecraft to space. Launch vehicle contains multiple stages, each of which contains a propulsion system. A typical liquid propellant rocket consists of a P.L.A., interstage, fuel tank, intertank, oxidizer tank, shroud and fin. The finite element model of the structure is modelled using MSC PATRAN. The structure is modelled as shell elements. Shell elements are 4-to-8-node iso parametric quadrilaterals or 3-to-6-node

triangular elements. Mesh size provided for all parts = 0.05m. The material used is steel with Young's modulus of $2x10^{11}$ N/m^2 and a density of 7280 kg/m^3.

- Modelling details of parts

5.1.1. PLA

A PLA of length 1 meter, thickness 0.1 meters and diameter 0.5 meters at one end and 1 meter at the other end is modelled.

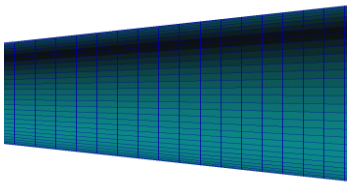

Fig. 1 F.E. model of P.L.A.

5.1.2. Propulsion for End Structure

Propulsion for end structure of 1-meter length, thickness 0.05 meter and 2-meter diameter is modelled.

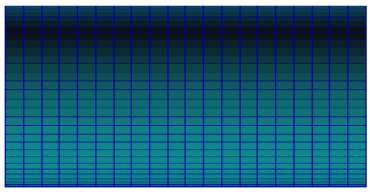

Fig. 2 F.E. model of inter stage

5.1.3. Fuel Tank

The fuel tank of thickness 0.05 meter, 10-meter length excluding dome and l meter diameter is modelled. At each 1-meter distance, an RB3 coupling is provided.

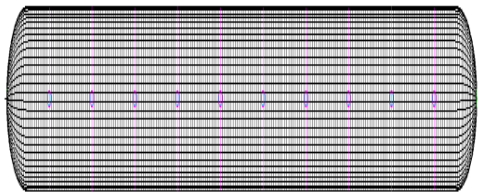

Fig. 3 F.E. model of fuel tank

5.1.4. Inter Tank

Inter tank of thickness 0.05 meter, 2-meter length and l meter diameter is modelled. At 1 meter distance, RB3 coupling is provided.

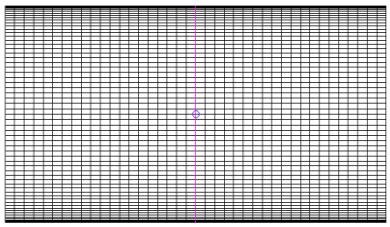

Fig. 4 F.E. model of inter tank

5.1.5. Oxidizer Tank

An oxidizer tank of thickness 0.05 meter, 10-meter length excluding dome and l meter diameter is modelled. At each 1-meter distance, an RB3 coupling is provided.

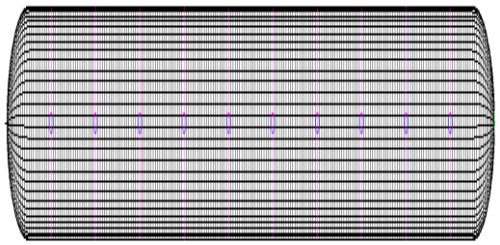

Fig. 5 F.E. model of oxidizer tank

5.1.6. Shroud

Shroud of thickness 0.1 meters, 5-meter length and l meter diameter is modelled. At each 1-meter distance, an RB3 coupling is provided, and a 2-meter length fin is modelled in four directions.

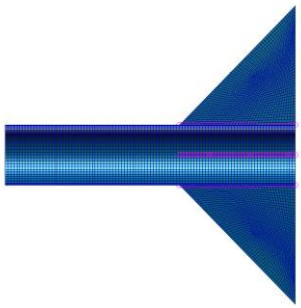

Fig. 6 F.E. model of the shroud

5.1.7. Fin

The fins at the bottom of a rocket provide stability. The 2-meter length fin is modelled in four directions around the bottom portion of the shroud.

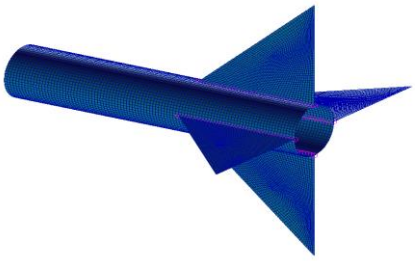

Fig. 7 F.E. model of shroud with fin

5.1.8. Propellant Modelling

The propellant is modelled as an equivalent spring-mass model in the lateral direction at the appropriate location. This propellant model is attached to the two center nodes where RB3 coupling is provided at the bottom portion of the fuel tank and oxidizer tank.

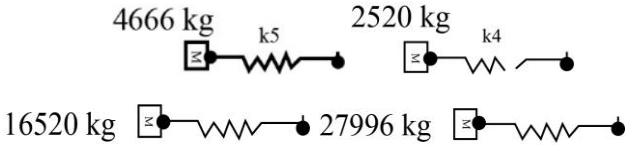

Fig. 8 Propellant model

5.1.9. Satellite Modelling

At the top of the Launch vehicle, i.e., at the top of P.L.A., RB2 coupling is provided. A 1000 kg satellite mass is connected to a spring. And this spring-mass system is

connected to the center node, where an RB2 coupling is provided at the top of P.L.A.

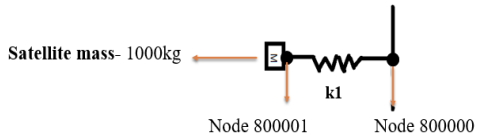

Fig. 9 Satellite model

5.1.10. Engine Modelling

An engine of mass 300kg modelled in the form of a mass-spring system is attached to the center node, where an RB3 coupling is provided at a distance of 2 meters from the top of the shroud part.

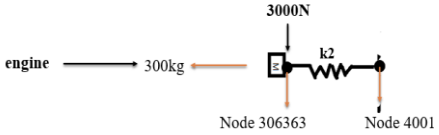

Fig. 10 Engine model

- Finite element model of the typical launch vehicle

A typical launch vehicle of 27.5-meter length and 1-meter diameter with and without propellant is modelled. RB2 coupling is used to connect the payload to the interstage, interstage to the fuel tank and fuel tank to the inter-tank, inter-tank to the oxidizer tank and oxidizer tank to the shroud. At 1 meter distance along the length of the fuel tank, intertank, oxidizer tank and shroud, RB3 coupling is provided. At the top of the Launch vehicle, i.e. at the top of the payload, RB2 coupling is provided, and a 1000 kg satellite in the form of a spring mass system is connected to the center node where an RB2 coupling is provided at the top of the payload. An engine of mass 300kg modelled in the form of a mass-spring system is attached to the center node, where an RB3 coupling is provided at a distance of 2 meters from the top of the shroud part. Table.1. shows the total mass of the launch vehicle without propellant.

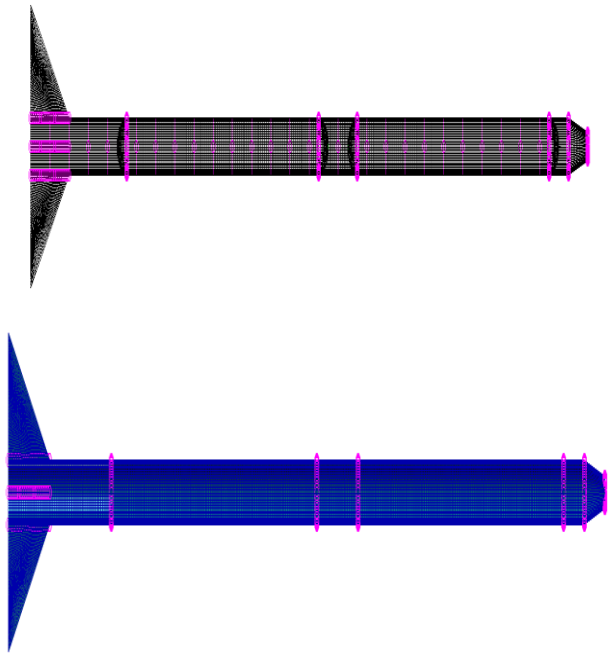

Fig. 11 F.E. model of a typical liquid propellant rocket

At node 400l, an engine in the form of a spring mass system is attached. 3000 N force is applied in the y direction, i.e., vertically downwards to node 306363, where a mass of 300kg is attached. At node 800000 (i.e. node at P.L.A. part), a spring mass system is provided. To this spring system, a satellite mass of 1000kg is attached. k1 is the stiffness of the spring where the satellite is attached. k2 is the stiffness of the spring where the engine is attached.

Propellant models are attached to the two center nodes where RB3 coupling is provided at the bottom portion of the fuel tank and oxidizer tank. In a liquid propellant rocket with propellant, k4 is the stiffness of the lower propellant mass in the fuel tank, and k5 is the stiffness of the lower propellant mass in the oxidizer tank. A liquid propellant rocket with the propellant model is shown in Figure 12

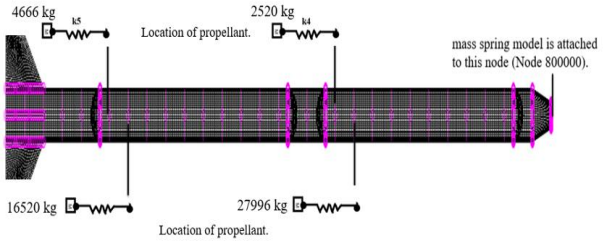

Fig. 12 F.E. model of launch vehicle with propellant

Table. 1 Mass of liquid propellant rocket with (a) without propellant (b)

(a)

Parts	Mass (kg)
Satellite	1000
PLA	3534.469
Interstage	2286.13
Fuel tank	12571.87
Fuel Propellant	27996
Inter tank	2286.13
Oxidizer tank	12571.87
Oxidizer Propellan	16520
Shroud	11430.65
Engine	300
Fin	2911.855
Total Mass	93408.97

(b)

Parts	Mass (kg)
Satellite	1000
PLA	3534.469
Interstage	2286.13
Fuel tank	12571.87
Inter tank	2286.13
Oxidizer tank	12571.87
Shroud	11430.65
Engine	300
Fin	2911.855
Total Mass	48892.97

6. Dynamic Analysis

6.1. Dynamic Characterization of Liquid Propellant Rocket with and Without Propellant

The first bending mode was found to be at 5.73 Hz for liquid propellant rockets without propellant and 5.35 Hz for liquid propellant rockets with propellant. The second bending mode was found to be at 20.37 Hz for liquid propellant rockets without propellant and 20.03 Hz for liquid propellant rockets with propellant. The first axial mode is found to be at 67.45 Hz for liquid propellant rockets without propellant and 46.42 Hz for liquid propellant rockets with propellant. The effect of propellant sloshing on certain locations of the launch vehicle is done by finding responses corresponding to the first bending modes.

Table. 2 Dynamic characterization of the liquid propellant rocket without propellant

Mode no.	Radians (Rad/sec)	Cycles (Hz)	Modes
1	0.00068	0.000108	Rigid body modes
2	0.000315	5.02E-05	Rigid body modes
3	0.000154	2.45E-05	Rigid body modes
4	0.000282	4.5E-05	Rigid body modes
5	0.000378	6.02E-05	Rigid body modes
6	0.000498	7.93E-05	Rigid body modes
7	36.03361	5.754927	1st bending mode
8	36.03368	5.754938	1st bending mode
9	107.1608	17.05517	torsion mode
10	107.1688	17.05644	torsion mode
11	119.6931	19.04975	torsion mode
12	127.9899	20.37022	2nd bending mode
13	128.014	20.37405	2nd bending mode
14	131.1138	20.8674	shell mode
15	217.6807	34.64496	3rd bending mode
16	217.6837	34.64543	3rd bending mode
17	283.1047	45.05751	torsion mode
18	360.4692	57.37045	4th bending mode
19	360.472	57.37091	4th bending mode
20	423.831	67.4548	1st axial mode

Table. 3 Dynamic characterization of liquid propellant rocket

Mode no.	Radians (Rad/sec)	Cycles (Hz)	Modes
1	0.000575	9.15E-05	Rigid body mode
2	0.000229	3.65E-05	Rigid body mode
3	0.00014	2.24E-05	Rigid body mode
4	0.000313	4.99E-05	Rigid body mode
5	0.000434	6.91E-05	Rigid body mode
6	0.000456	7.26E-05	Rigid body mode
7	33.64024	5.35401	1st bending mode
8	33.64032	5.354024	1st bending mode
9	86.7081	13.80002	fin mode
10	86.70996	13.80032	Fin mode
11	119.6931	19.04975	fin mode
12	125.8662	20.03223	2nd bending mode
13	125.8965	20.03704	2nd bending mode
14	131.1137	20.8674	fin mode
15	168.271	26.78116	3rd bending mode
16	168.2719	26.7813	3rd bending mode
17	283.1047	45.05751	torsion mode
18	291.666	46.42009	1st axial mode
19	300.5196	47.82918	4th bending mode
20	300.5214	47.82947	4th bending mode

Table. 4 Dynamic characterization of the slosh model

Mode No.	Radians (Rad/sec)	Cycles (Hz)
1	6.642973E-04	1.057262E-04
2	2.776092E-04	4.418287E-05
3	2.040673E-04	3.247832E-05
4	9.487526E-05	1.509987E-05
5	2.695650E-04	4.290260E-05
6	3.375440E-04	5.372180E-05
7	3.051583E+01	4.856745E+00
8	3.199138E+01	5.091587E+00
9	3.311882E+01	5.271024E+00
10	3.364028E+01	5.354016E+00
11	3.635964E+01	5.786817E+00
12	8.670903E+01	1.380017E+01
13	9.143440E+01	1.455224E+01
14	1.196931E+02	1.904975E+01
15	1.242586E+02	1.977637E+01
16	1.258814E+02	2.003465E+01
17	1.286079E+02	2.046858E+01
18	1.311137E+02	2.086740E+01
19	1.682714E+02	2.678123E+01
20	1.843193E+02	2.933533E+01

6.2. Transient Analysis

- Acceleration at nodes where satellite and engine are attached

At node 400l, an engine is attached. 3000 N force is applied in the y direction, i.e., vertically downwards to node 306363, where a mass of 300kg is attached. A spring-mass system is provided at node 800000 (i.e. node at P.L.A. part). To this spring system, a satellite mass of 1000kg is attached. When thrust is applied to the motor (at node 306363), the response at node 800001(node where satellite mass is attached) and node 306363(node where the motor is attached) is taken. 1st bending mode of the launch vehicle with and without propellant was found to be at 5.35 Hz and 5.73 Hz. Firstly the spring is stiffened. Then the stiffness is varied. k1 is the stiffness of the spring where the satellite is

attached, k2 is the stiffness of the spring where the engine is attached, and k3 is the excitation force applied at a time interval of 0.01 to 35 seconds. In liquid propellant rocket with propellant. k4 is the stiffness of the lower mass of propellant in the fuel tank, and k5 is the stiffness of the lower mass of propellant in the oxidizer tank. Transient analysis is done by changing the stiffness of two propellants.

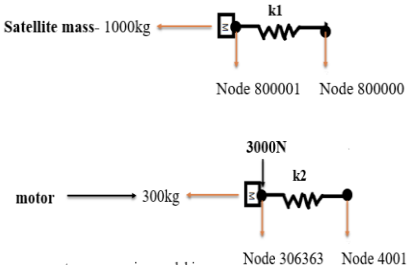

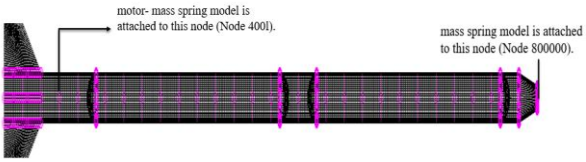

Fig. 15 Liquid propellant rocket without propellant

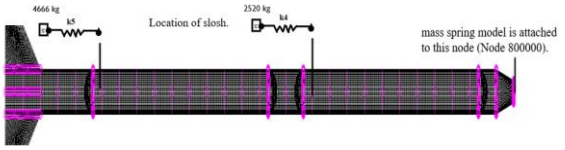

Fig. 16 Liquid propellant rocket with propellant

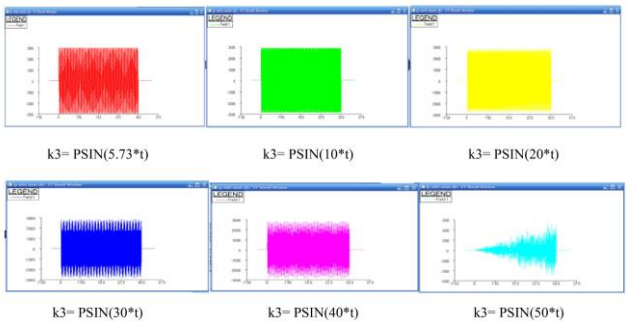

Fig. 17 Excitation force applied at engine gimbal point

6.2.1. Responses at the Satellite of a Liquid Propellant Rocket with Propellant

Case 1: k1 rigid, k3 constant = 5.35 Hz, k2 varying

• Excitation force applied at engine gimbal point - k3= Psin(5.35*t)

• Response:

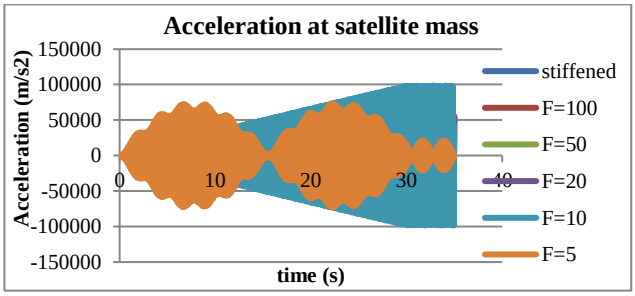

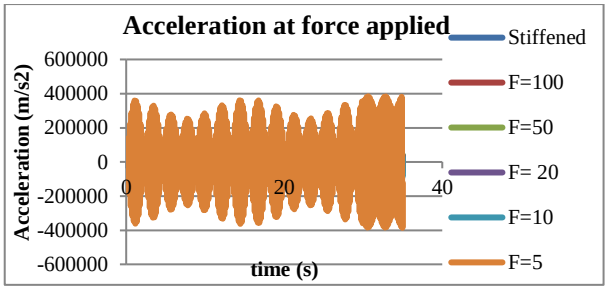

Fig. 18 Graph showing acceleration response at satellite and force applied nodes obtained from analysis of launch vehicle with propellant

Case 2: k1 rigid, k3 varying, k2 rigid

- Excitation force applied at engine gimbal point- k3= PSin(5.35,10,20,30,40,50*t)
- Responses:

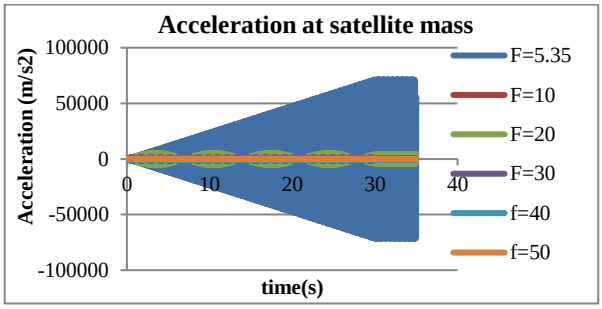

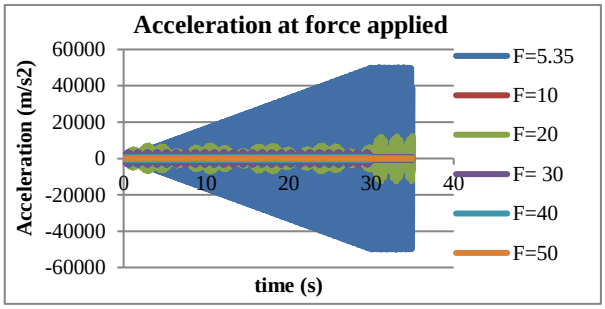

Fig. 19 Graph showing acceleration response at satellite and force applied nodes obtained from analysis of launch vehicle with propellant

- Case 3: k2 rigid, k3 varying, k1 varying
- Excitation force applied at engine gimbal point - k3= PSin(5.35,10,20,30,40,50*t)
- Responses:

Response at satellite and force applied nodes obtained from analysis of launch vehicle with propellant without sloshing -:

k1= 100 Hz

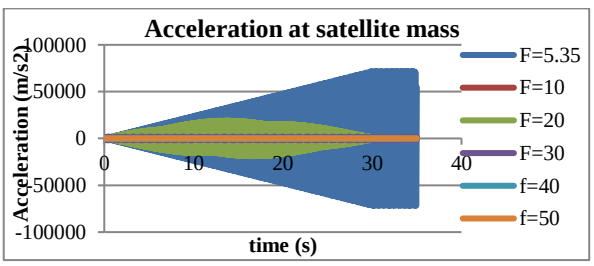

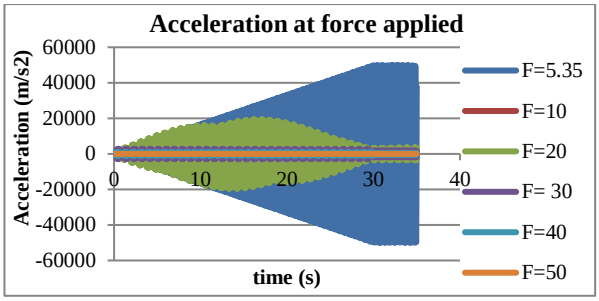

k1= 50 Hz

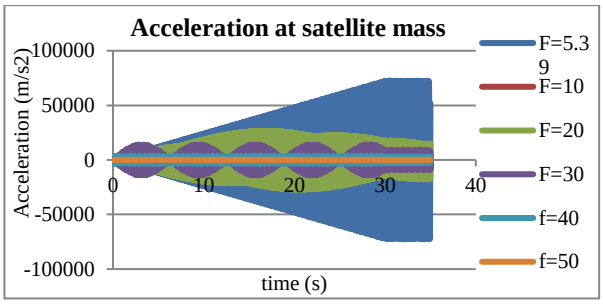

k1= 5 hz

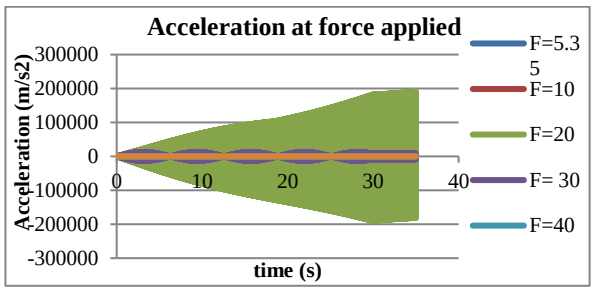

k1= 20 Hz

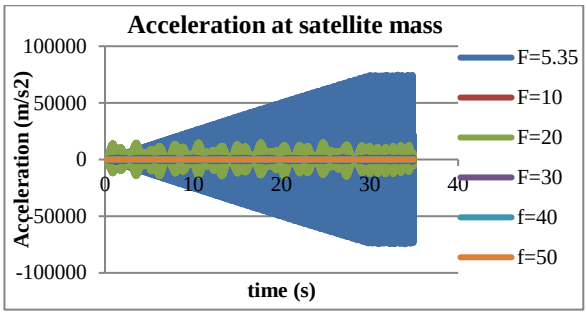

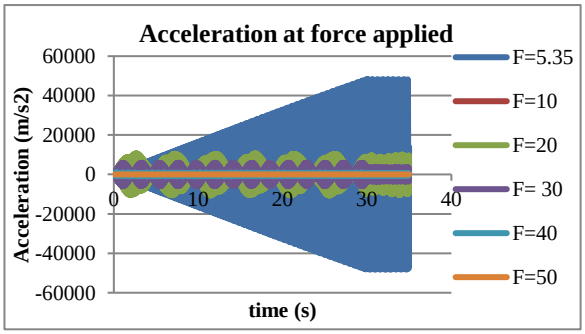

k1= 10 hz

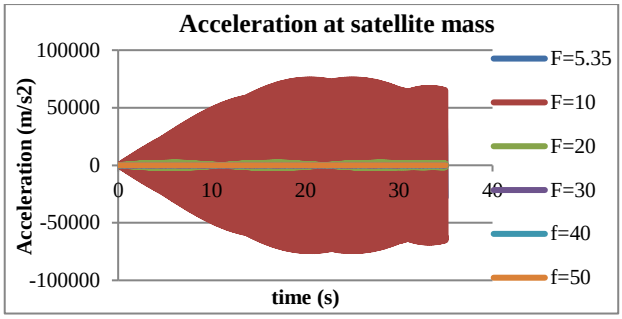

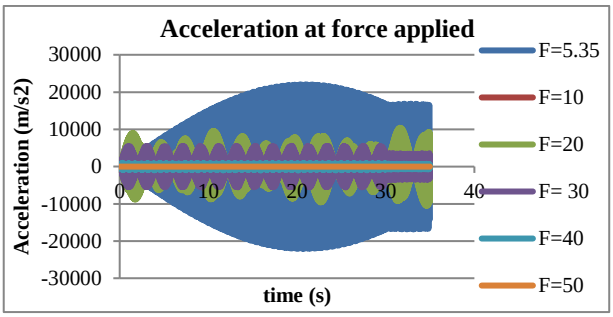

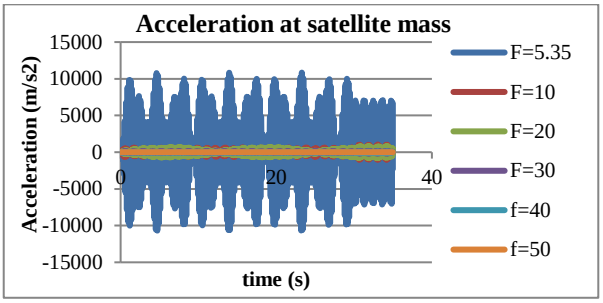

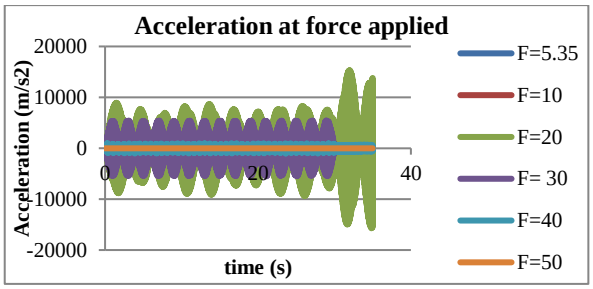

Fig. 20 Graph showing acceleration response at satellite and force applied nodes obtained from analysis of launch vehicle with propellant.

- Case 4: k4 varying, k5 rigid, k1=5.13Hz, k2=20 Hz and k4 rigid, k5 varying, k1=5.13Hz, k2=20 Hz
- Excitation force applied at engine gimbal point- k3= PSin(5.73, 20, 10*t)
- Response:

Graph showing acceleration response at satellite and force applied nodes obtained from analysis of launch vehicle with propellant sloshing -:

- k4 varying, k5 rigid, k1=5.13Hz, k2=20 Hz

k3=5 Hz

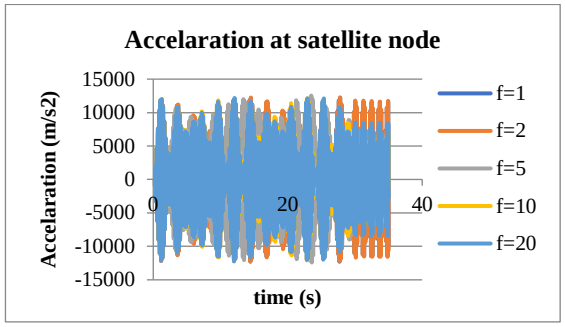

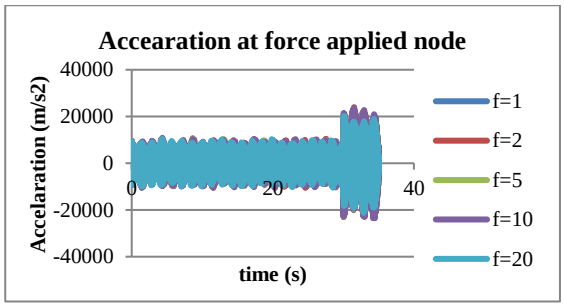

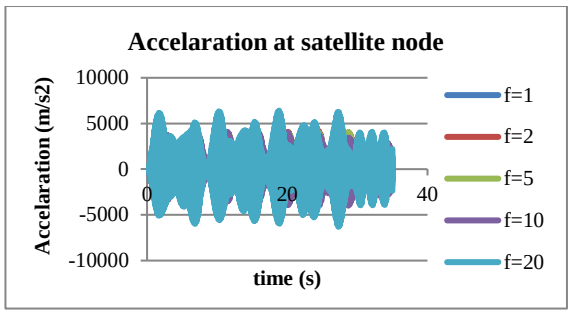

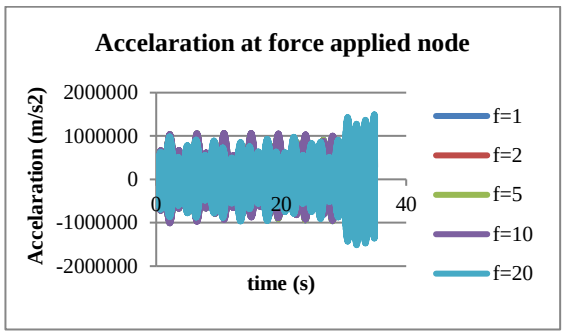

k3= 30 hz

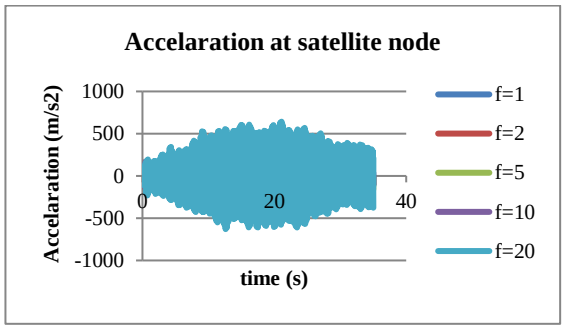

k3= 30 hz

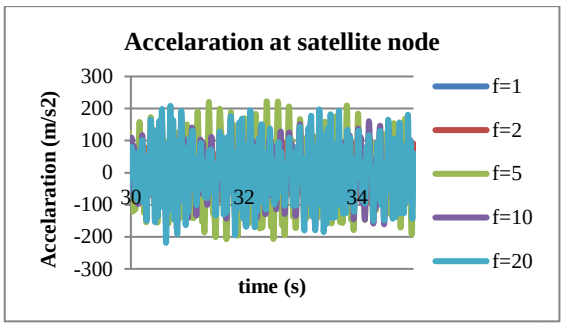

Fig. 21 Graph showing acceleration response at satellite and force applied nodes obtained from analysis of launch vehicle with propellant sloshing.

- k4 rigid, k5 varying, k1=5.13Hz, k2=20 Hz

k3=5 Hz

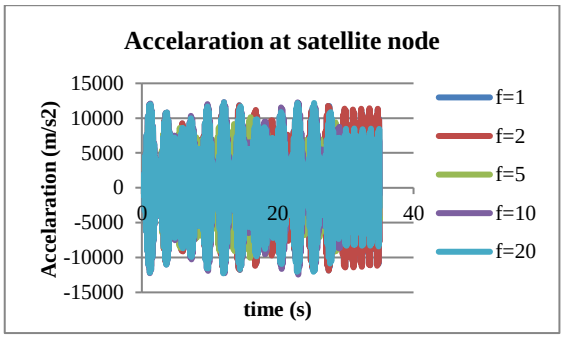

k3= 20 hz

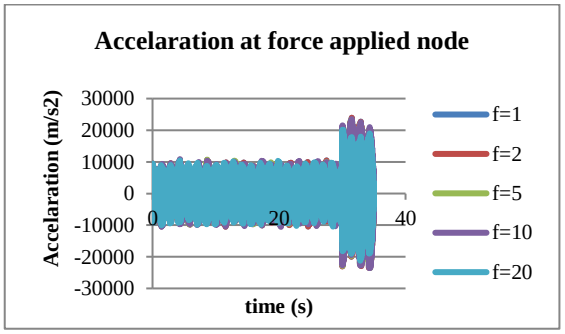

k3= 20 hz

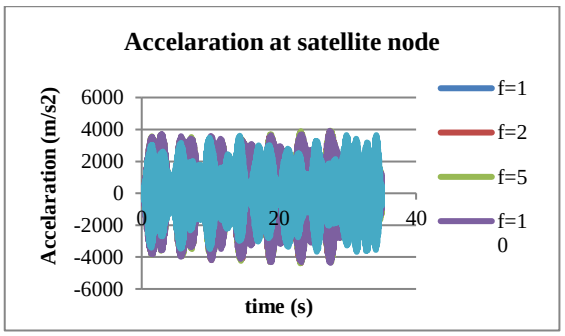

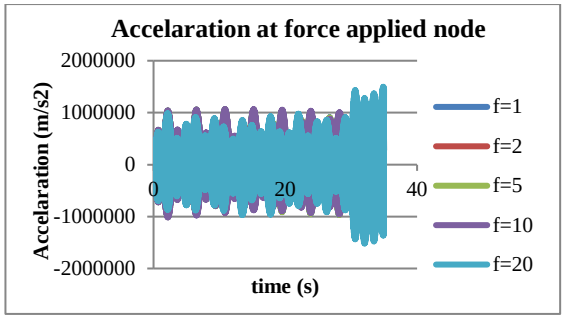

k3= 30 hz

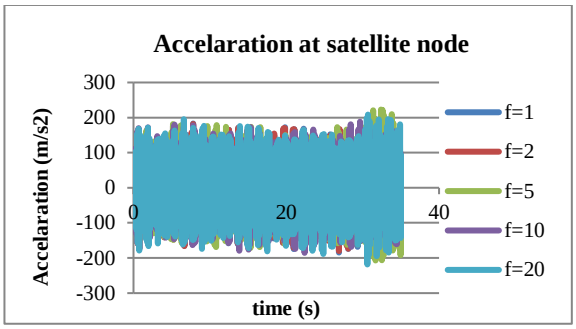

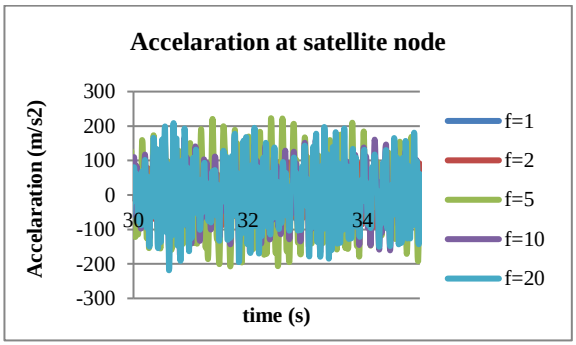

Fig. 22 Graph showing acceleration response at satellite and force applied nodes obtained from analysis of launch vehicle with propellant sloshing

6.3. Discussions

- For case 1, k1 stiffened k2 varying, k3=5.35 Hz. The stiffness of the spring where the engine is attached, i.e. k2 with f=10 Hz, is found to have a greater response at the node where the satellite is attached, as shown in Figure 18. Therefore it can be concluded that the response is greater when the frequency of the spring where the engine is attached is near the structural frequency of the launch vehicle with propellant.

- For case 2: k1 stiffened, k2 stiffened, applied excitation with stiffness f=5.75 Hz is found to be having a greater response at the node where the satellite is attached, as shown in Figure 6.7 and Table 6.4. Therefore it can be concluded that the response is more when the frequency of applied excitation force is near the structural frequency for the launch vehicle with propellant.

- In case 3, for k3=5.35 Hz, Spring with k1=5Hz is found to be having a greater response at the node where force is applied. The response is more when the frequency is near the structural frequency for the launch vehicle with propellant.

- When sloshing occurs, i.e. in case 4, when k4 is varying, and k5 is rigid, for k3=5.35Hz, k4=5Hz shows greater response, k3=20Hz, k4= 20Hz shows greater response, k3= 30Hz, k4=20Hz shows the greater response at the node where the satellite is attached and at the node where force is applied, k3=5.35Hz, k4=1Hz shows greater response, k3=20Hz, k4= 20Hz shows greater response, k3= 30Hz, k4=1Hz shows greater response as seen in Figure 20. When k4 is rigid, and k5 is varying, for k3=5.35Hz, k5=10Hz shows greater response, k3=20Hz, k5=5Hz shows greater response, k3= 30Hz, k5=5Hz shows the greater response at the node where the satellite is attached and at the node where force is applied, when k3=5.35Hz, k5=2Hz shows greater response, k3=20Hz, k5= 20Hz shows greater response, k3= 30Hz, k5=20Hz shows greater response as seen in Figure 21. From this result, it is clear that the location of propellant, slosh frequencies, and sloshing will cause response changes at specified locations, i.e. at nodes where the satellite is attached and at nodes where force is applied. And it is seen that as sloshing occurs, vibration has reduced for case 4.

7. Conclusion

Launch vehicles are used to carry spacecraft to space. Launch vehicle contains multiple stages, each of which contains a propulsion system. A liquid rocket propulsion system typically consists of an engine, fuel tanks, and a vehicle frame to hold everything in place while connecting to the payload and launch pad. It is common knowledge that the sloshing of liquid propellants can disrupt the spacecraft's control system. Hence, the issue of sloshing dynamics is becoming more significant. A typical launch vehicle with and without propellant was modelled, and dynamic analysis was carried out. Dynamic analysis includes structural characterization and transient analysis of the launch vehicle with and without propellant. From the modal analysis done, the first bending mode was found to be at 5.75Hz for the launch vehicle without propellant and 5.35Hz for the launch vehicle with propellant. With respect to these frequencies, transient analysis was carried out, i.e., the effect of propellent and propellant sloshing on the structure. Analysis was done by taking different cases. It is seen that the response is more when the frequency of applied excitation force is near the structural frequency for the launch vehicle with propellant. And when propellant sloshing occurs, it is seen that frequency of excitation force is near to sloshing frequency. It is also evident from the graphs that vibration has reduced as sloshing occurs, and the acceleration response has reduced. Thus indicating that slosh is a good vibration absorber and acts as a good damper. Therefore, it is clear that based on the location of the propellant, slosh frequencies and sloshing will cause changes in responses at satellite locations. It can be concluded that based on structural frequencies, location of force applied, and location of the propellant model connected, slosh frequencies can cause changes in responses at the satellite location of a launch vehicle and thus, the effect of coupling between the propellant sloshing and the vehicle modes are studied.

References

[1] James M. Adler, Michael S. Lee, and John D. Saugen, "Adaptive Control of Propellant Slosh for Launch Vehicles," *Sensors and Sensor Integration*, vol. 1480, 1991. [CrossRef] [Google Scholar] [Publisher Link]

[2] M. Chiba, and H. Magata, "Coupled Pitching Dynamics of Flexible Space Structures with On-board Liquid Sloshing," *Acta Astronautica*, vol. 181, pp. 151-166, 2021. [CrossRef] [Google Scholar] [Publisher Link]

[3] Sangbum Cho, M. McClamroch, and Mahmut Reyhanoglu, "Feedback Control of a Space Vehicle with Unactuated Fuel Slosh Dynamics," *AIAA Guidance, Navigation, and Control Conference and Exhibit*, 2000. [CrossRef] [Google Scholar] [Publisher Link]

[4] L. Constantin et al., "Nonlinear Damping Effects in Vertically Vibrating Systems with Violently Sloshing Liquid," *Journal of Sound and Vibration*, vol. 544, p. 117405, 2023. [CrossRef] [Google Scholar] [Publisher Link]

[5] De-Lin Cui et al., "Parametric Resonance of Liquid Sloshing in Partially Filled Spacecraft Tanks during the Powered-flight Phase of Rocket," *Aerospace Science and Technology*, vol. 35, pp. 93-105, 2014. [CrossRef] [Google Scholar] [Publisher Link]

[6] Paolo Gasbarri, Marco Sabatini, and Andrea Pisculli, "Dynamic Modelling and Stability Parametric Analysis of a Flexible Spacecraft with Fuel Slosh," *Acta Astronautica*, vol. 127, pp. 141-159, 2016. [CrossRef] [Google Scholar] [Publisher Link]

[7] R.A. Ibrahim, V.N. Pilipchuk, and T. Ikeda, "Recent Advances in Liquid Sloshing Dynamics," Applied Mechanics Reviews, vol. 54, no. 2, pp. 113-119, 2001. [CrossRef] [Google Scholar] [Publisher Link]

[8] Abdol M. Khoshnood et al., "Dynamic Modeling and Controller Design for a Space Vehicle with Fuel Sloshing," *Journal of Solid and Fluid Mechanics*, vol. 11, no. 2, pp. 25-40, 2021. [CrossRef] [Google Scholar] [Publisher Link]

[9] Dong Hyun Kim, and Jae Weon Choi, "Attitude Controller Design for a Launch Vehicle with Fuel-slosh," *SICE 2000. Proceedings of the 39th SICE Annual Conference, International Session Papers*, 2000. [CrossRef] [Google Scholar] [Publisher Link]

[10] Marcos Chimeno Manguan et al., "Dynamic Coupling on the Design of Space Structures," *Aerospace Science and Technology*, vol. 84, pp. 1035-1048, 2019. [CrossRef] [Google Scholar] [Publisher Link]

[11] Kriti Telang, and Dinesh Chand Gupta, "Improved Latch Type Modified Sense Amplifier for Suppress Coupling," *SSRG International Journal of VLSI & Signal Processing*, vol. 6, no. 2, pp. 1-4, 2019. [CrossRef] [Publisher Link]

[12] M.A. Noorian, H. Haddadpour, and M. Ebrahimian, "Stability Analysis of Elastic Launch Vehicles with Fuel Sloshing in Planar Flight using a BEM-FEM Model," *Aerospace Science and Technology*, vol. 53, pp. 74-84, 2016. [CrossRef] [Google Scholar] [Publisher Link]

[13] ZhongWen Pan et al., "Liquid Propellant Analogy Technique in Dynamic Modeling of Launch Vehicle," *Science China Technological Sciences*, vol. 53, pp. 2102-2110, 2010. [CrossRef] [Google Scholar] [Publisher Link]

[14] M. Reyhanoglu, "Maneuvering Control Problems for a Spacecraft with Unactuated Fuel Slosh Dynamics," *Proceedings of 2003 IEEE Conference on Control Applications*, 2003. [CrossRef] [Google Scholar] [Publisher Link]

[15] V. Ramesh Babu et al., "Down Stream Fault Current Interruption by Dynamic Voltage Restorer," *SSRG International Journal of Electrical and Electronics Engineering*, vol. 1, no. 7, 2014. [CrossRef] [Publisher Link]

[16] Hesham Shageer, and Gang Tao, "Modeling and Adaptive Control of Spacecraft with Fuel Slosh: Overview and Case Studies," *AIAA Guidance, Navigation and Control Conference and Exhibit*, 2007. [CrossRef] [Google Scholar] [Publisher Link]

[17] Jiangtao Xu et al., "Modeling and Analysis of Long Booster Clustered Launch-vehicle," *Scientific Reports*, vol. 10, 2020. [CrossRef] [Google Scholar] [Publisher Link]

[18] Dewei Zhang et al., "Modeling and Analysis of Aeroelasticity and Sloshing for Liquid Rocket," *IEEE Access*, vol. 7, pp. 4453-4465, 2018. [CrossRef] [Google Scholar] [Publisher Link]

[19] Honghua Zhang, and Zeguo Wang, "Attitude Control and Sloshing Suppression for Liquid-filled Spacecraft in the Presence of Sinusoidal Disturbance," *Journal of Sound and Vibration*, vol. 383, pp. 64-75, 2016. [CrossRef] [Google Scholar] [Publisher Link]

[20] K.S. Rao, and Prashanthan, "Ground Wind Response of Launch Vehicles with Liquid Propellant – Slosh as a Dynamic Vibration Absorber," *Proceedings of 48th AGM*, 1997.

[21] Mahmut Reyhanoglu, "Modeling and Control of Space Vehicles with Fuel Slosh Dynamics," 2011. [Google Scholar] [Publisher Link]

[22] Elena Sierikova et al., "*Coupled Boundary and Finite Element Method for Stability Analysis of Launch Vehicle*," Doctoral Dissertation, IKSAD Publications, 2023. [Google Scholar] [Publisher Link]

[23] Sudermann. E.J, Gangadharan. N.S, Marsell. B, "CFD Fuel Motorling of Fluid Structure Interaction in Spacecraft Propellant Tanks with Diaphragms," ntrs.nasa.gov/api/citations.

[24] Roy R. Craig, and Andrew J. Kurdila, *Fundamentals of Structural Dynamics*, John Wiley & Sons, 2006. [Google Scholar] [Publisher Link]

[25] George P. Sutton, *History of Liquid Propellant Rocket Engines*, American Institute of Aeronautics and Astronautics, 2006. [Google Scholar] [Publisher Link]

[26] Launchers. [Online]. Available: https://www.isro.gov.in/Launchers.html

[27] Design and Integration Tools. [Online]. Available: https://software.nasa.gov/software/LAR-16804-GS
Liquid Rocket Engine. [Online]. Available: https://www.grc.nasa.gov/www/k-12/airplane/lrockth.html